

# Quantum and frustration effects on fluctuations of the inverse compressibility in two-dimensional Coulomb glasses

Minchul Lee,<sup>1</sup> Gun Sang Jeon,<sup>2</sup> and M. Y. Choi<sup>1,3</sup>

<sup>1</sup>Department of Physics, Seoul National University, Seoul 151-747, Korea

<sup>2</sup>Center for Strongly Correlated Materials Research,  
Seoul National University, Seoul 151-747, Korea

<sup>3</sup>Korea Institute for Advanced Study, Seoul 130-012, Korea

We consider interacting electrons in a two-dimensional quantum Coulomb glass and investigate by means of the Hartree-Fock approximation the combined effects of the electron-electron interaction and the transverse magnetic field on fluctuations of the inverse compressibility. Proceeding systematic study of the system in the absence of the magnetic field identifies the source of the fluctuations, interplay of disorder and interaction, and effects of hopping. Revealed in sufficiently clean samples with strong interactions is an unusual right-biased distribution of the inverse compressibility, which is neither of the Gaussian nor of the Wigner-Dyson type. While in most cases weak magnetic fields tend to suppress fluctuations, in relatively clean samples with weak interactions fluctuations are found to grow with the magnetic field. This is attributed to the localization properties of the electron states, which may be measured by the participation ratio and the inverse participation number. It is also observed that at the frustration where the Fermi level is degenerate, localization modulation of electrons is enhanced, raising fluctuations. Strong frustration in general suppresses effects of the interaction on the inverse compressibility and on the configuration of electrons.

PACS numbers: 73.23.Hk, 71.55.Jv, 71.30.+h

## I. INTRODUCTION

Since the experimental observation of the crucial effects of the Coulomb interaction,<sup>1</sup> mesoscopic fluctuations of the inverse compressibility in two-dimensional quantum dots have been investigated intensively, both theoretically and experimentally.<sup>1,2,3,4,5,6,7,8,9,10</sup> Recent experiments<sup>1,2,3</sup> on the distribution of the inverse compressibility, which can be measured by conductance peak spacing, in the Coulomb-blockade regime have shown that the standard random matrix theory fails to explain the observed fluctuations; this implies that charging energy fluctuations may play a dominant role in the inverse-compressibility fluctuations. In particular, the distribution was observed to take a Gaussian-like symmetric form with non-Gaussian tails.<sup>1,2,3</sup> Subsequent analytical and numerical studies on interacting electrons in disordered systems revealed the possibility of larger inverse-compressibility fluctuations induced by Coulomb interactions.<sup>1,4,5,6,7,8</sup> It was also proposed that the shape deformation of the dot due to the gate-voltage sweeping<sup>9</sup> or the irregular shape of the dot<sup>10</sup> may contribute to the deviation of the experimental results from the Wigner-Dyson (WD) statistics predicted by the random matrix theory. However, the recent experiment with a stacked gate structure, which allows one to vary the electron density without significant deformation of the dot, was supportive of the claim that the observed shape of fluctuations originates from electron-electron interactions.<sup>2</sup> Another recent experiment reported the crossover behavior of the compressibility around the metal-insulator transition in two dimensions.<sup>11</sup>

The influence of the magnetic field, either perpendicular<sup>1,3</sup> or parallel,<sup>12</sup> on the distribution

of the inverse compressibility was also investigated experimentally. In the presence of a perpendicular magnetic field, the shape of the distribution is found qualitatively similar to that in zero magnetic field, only with narrower width.<sup>3</sup> There was an attempt to explain the qualitative behavior of peak positions in the system under the magnetic field;<sup>3</sup> the considered classical model is based on the electrostatics of several electron islands with quantum orbitals, the energies of which depend on the external magnetic field. The possibility of nearly vanishing peak spacing was thus suggested, which is in qualitative agreement with the bunching of the addition spectra.<sup>14</sup> However, it does not take into account the quantum interference effects between electron wave functions, which can be crucial in mesoscopic systems.

In this paper, we study numerically fluctuations of the inverse compressibility in the two-dimensional Coulomb glass.<sup>15,16,17</sup> To treat the interaction between electrons, we employ the Hartree-Fock (HF) approximation, which makes it possible to investigate larger samples than those feasible in exact diagonalization. For a systematic study, we first examine the classical system, revealing the detailed dependence of the inverse-compressibility fluctuations upon disorder and interaction. Then the effects of electron hopping on the fluctuations are investigated. Observed is an unusual right-biased distribution for very weak disorder and strong interactions as well as a symmetric Gaussian-like distribution with non-Gaussian tails. It is also found that relative fluctuations decrease eventually for sufficiently strong interactions, which appears to be inconsistent with the quadratic interaction dependence of the fluctuations suggested in a previous numerical study.<sup>8</sup> We further examine the effects of mag-

netic elds, which introduce frustration to the system, on the distributions and fluctuations of the inverse compressibility, and observe that weak magnetic elds tend to suppress fluctuations. Nevertheless the fluctuations may be enhanced in some range of the frustration for weak disorder and interaction. Such opposite tendency of the inverse-compressibility fluctuations in response to the applied magnetic elds is explained in terms of the localization properties of the system. Finally, it is also found that strong frustration suppresses significantly the effects of the interaction.

This paper is organized as follows: In Sec. II we consider the classical Coulomb glass and investigate in detail the effects of disorder and interaction on the inverse-compressibility fluctuations. The effects of hopping on the fluctuations in the quantum Coulomb glass are examined in Sec. III. Section IV is devoted to the effects of magnetic elds. We examine the system at both weak and strong frustration, and describe the electron distributions and localization properties by means of the participation ratio and the inverse participation number. The main results are summarized in Sec. V.

## II. CLASSICAL COULOMB GLASS

We address the Hamiltonian for the classical Coulomb glass model:<sup>15</sup>

$$H = \sum_i w_i \hat{n}_i + \frac{1}{2} \sum_{i \neq j} (\hat{n}_i - K) U_{ij} (\hat{n}_j - K); \quad (1)$$

where  $i$  is the site index on an  $L \times L$  square lattice,  $\hat{n}_i$  is the number operator of the electron at site  $i$ , and  $w_i$  is the random on-site potential uniformly distributed in the range  $[-W; W]$ . We assume the Coulomb interaction potential between electrons:

$$U_{ij} = \frac{e^2}{\epsilon_0 \epsilon_r |r_i - r_j|} - \frac{V}{|r_i - r_j|} \quad (2)$$

with  $\epsilon_r$  being the dielectric constant. In Eq. (1)  $K$  represents the uniform neutralizing background charge per site in units of  $+e$ , which is demanded by the charge neutrality condition over the whole system. Throughout this paper we concentrate on the half-filling case  $K = 1/2$  in the free boundary conditions, and write the distance in units of the lattice constant  $a$ .

The ground state of the classical Hamiltonian in Eq. (1) is obtained by means of simulated annealing procedure. The inverse compressibility  $\chi_2$  for a given disorder configuration is then calculated via the relation

$$\chi_2 = E_{M+1} - 2E_M + E_{M-1}; \quad (3)$$

where  $M = L^2/2$  and  $E_n$  denotes the  $n$ -electron ground-state energy. We have performed the calculation for size  $L = 4, 6$ , and  $8$ , and averaged the data over 2000 different disorder configurations.

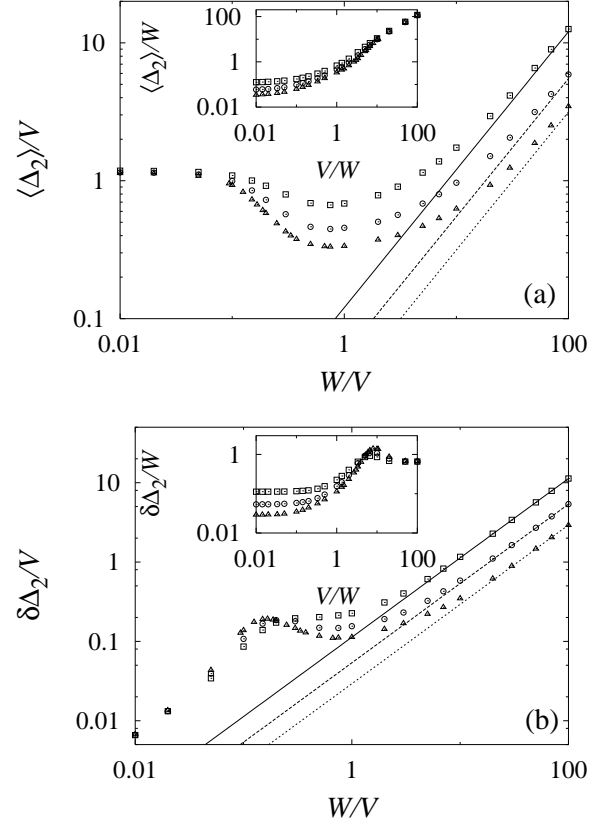


FIG. 1: (a) Averages and (b) fluctuations of the inverse compressibility in units of  $V$  as functions of  $W/V$  in the classical system of size  $L = 4$  ( $\square$ ),  $6$  ( $\circ$ ), and  $8$  ( $\triangle$ ). Each straight line represents the behavior of the corresponding noninteracting system ( $V = 0$ ). The insets display the averages and the fluctuations in units of  $W$  as functions of  $V/W$ .

Figure 1(a) shows the average inverse compressibility as a function of the relative disorder strength  $W/V$ . For weak disorder,  $\langle \chi_2 \rangle = V$  depends rather weakly on both the disorder strength  $W$  and the size  $L$  since  $\langle \chi_2 \rangle$  is proportional to  $V$  in this regime as shown in the inset. As the disorder is increased,  $\langle \chi_2 \rangle = V$  is suppressed up to  $W/V = 1$ , then increases for  $W/V > 1$ , and approaches asymptotically the straight line describing the behavior in the corresponding noninteracting system. One can also observe that  $\langle \chi_2 \rangle$  decreases with the system size, which is prominent for strong disorder. It is remarkable that the disorder-scaled average  $\langle \chi_2 \rangle = W$ , which is plotted in the inset of Fig. 1(a), is monotonically increasing with  $V/W$ , thus indicating that larger interactions lead to larger values of the inverse compressibility for given disorder strength.

In contrast to the average  $\langle \chi_2 \rangle$ , the fluctuations  $\delta \chi_2$  of the inverse compressibility, shown in Fig. 1(b), scale with  $W$  independently of  $V$  for weak disorder as well as for strong disorder. In the crossover regime, on the other hand, the fluctuations display non-monotonic behavior, with a broad peak at  $W/V \approx 0.2$ . This becomes conspic-

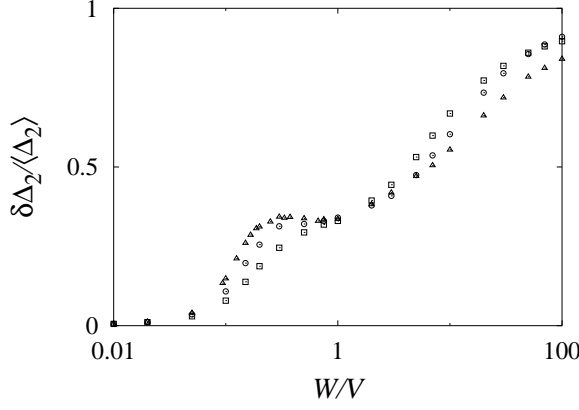


FIG. 2: Relative fluctuations versus  $W/V$  in the classical system. The symbols are the same as those in Fig. 1.

uous as the system size grows:  $W$  hereas for  $W/V > 0.2$ ,  $\delta_2$  decreases with the size similarly to  $h_{2i}$ , slight increase of  $\delta_2$  can be observed for  $W/V \leq 0.2$ . It is of interest to note that  $\delta_2$  approaches the noninteracting limit rather fast as  $W/V$  is increased, demonstrating that for strong disorder ( $W/V \rightarrow 1$ ) the interaction merely shifts the average inverse compressibility toward slightly larger values.

In Fig. 2 we plot the relative fluctuations  $\delta_2 = h_{2i}$  of the inverse compressibility versus the relative disorder strength  $W/V$ . The relative fluctuations in general grow with  $W/V$ , saturating to a finite value in the noninteracting limit. At the point  $W/V = 1$  the relative fluctuations are apparently independent of the system size, which has been reported in previous numerical studies.<sup>6,7</sup> However, it should be noted that such universal behavior shows up only at  $W/V = 1$ : While the relative fluctuations grow with the system size for  $W/V \leq 1$ , they are reduced by the increase of the system size for  $W/V \geq 1$ . Again a broad peak, which becomes prominent for larger systems, is observed for  $W/V \approx 0.2$ ; this can be attributed to the presence of the peak in  $\delta_2$  mentioned above.

In the limit of strong disorder ( $W/V \rightarrow 1$ ), the electrons are distributed spatially to minimize the total random potential energy, and are pinned, rarely rearrange their whole distribution in response to the addition or removal of an electron. Consequently, as in the noninteracting system, both  $h_{2i}$  and  $\delta_2$  are expected to increase with the disorder strength  $W$ , while the interaction simply renormalizes the values slightly without qualitative change. Note that such tendency begins at relatively small disorder  $W/V \approx 0.1$ , as shown in Fig. 1.

In the opposite limit of strong interaction ( $W/V \rightarrow 1$ ), on the other hand, the half-filled electron state  $\mathcal{M}_i$  is expected to form a Wigner crystal (WC). In case that two WC states are nearly degenerate even in the presence of the disorder, the addition or removal of an electron can change the ground state into that similar to the other WC state; however, the disorder configuration, which allows

such phenomena, is very rare and accordingly, the WC state in general does not experience significant change by the insertion or extraction of an electron. The inverse compressibility can then be calculated as follows:

$$\begin{aligned} \chi^{-1} &= (E_M + 1) \chi(E_M) + (E_M - 1) \chi(E_M) \\ &= w_{i+} + (n_i - K) U_{ii+} - w_{i-} + (n_i - K) U_{ii-} \\ &= w_{i+} - w_{i-} + \sum_i (n_i - K) (U_{ii+} - U_{ii-}); \end{aligned} \quad (4)$$

where  $n_i$  is 0/1 for site  $i$  empty/occupied in the state  $\mathcal{M}_i$ , and  $i$  represents the site to/from which an electron is inserted/extracted. In this limit, the interaction part plays a major role in choosing  $i$ , which is very likely to be one of the corners. Accordingly, the strength  $w_i$  of the impurity at site  $i$  is random and uncorrelated, leading to the disorder-independent average given by the third term on the right-hand side of Eq. (4); this quantity decreases slightly with  $L$ . In contrast, the fluctuations arise mainly from the first two terms which have their origin in the random potential and thus increase with the disorder strength  $W$ . The numerical data presented above are indeed in good agreement with these conclusions based on analytic argument. Figure 1 demonstrates that this regime persists until  $W/V \approx 0.2$ .

In both extreme limits considered above, one can see that the contributions of the random potential to the fluctuations of the inverse compressibility are dominant over those of the interaction. In the intermediate region, however, the behavior looks rather complicated and the interaction is expected to play an important role. For detailed investigation, we divide the intermediate region into three subregions: (I)  $0.02 < W/V < 0.2$ , (II)  $0.2 < W/V < 0.5$ , and (III)  $0.5 < W/V < 1$ . In Region I the half-filled state  $\mathcal{M}_i$  strongly depends on the disorder configuration: Some states are still close to the WC state while others are rather disordered. In the latter states, the portion of which increases with  $W/V$ , the distribution of electrons is inhomogeneous, reducing the Coulomb energy cost of the addition or removal of one electron. On the other hand, the former states, which resemble the WC state, rather easily rearrange the distribution of electrons by the addition or removal of an electron, unlike in the limit of strong interactions. Both behaviors generally result in the reduction of  $\delta_2$  although the amount of the reduction depends upon the disorder configuration; this explains the change of the  $\delta_2 = V$  distribution from the  $\delta$ -function-like one [see Fig. 3(a)] to the asymmetric broad distribution with a long left tail [see Fig. 3(b)]. It is observed that the minimum of  $\delta_2 = V$  as well as the peak position of the distribution decreases with  $W/V$ . Indeed in a finite system the minimum of  $\delta_2 = V$  hits its lower bound given by the smallest possible Coulomb interaction between successively inserted electrons,<sup>6</sup>

$$\frac{\delta_2^{\min}}{V} = \frac{1}{\epsilon_{\max}} = \frac{1}{(L-1)^2} \quad (5)$$

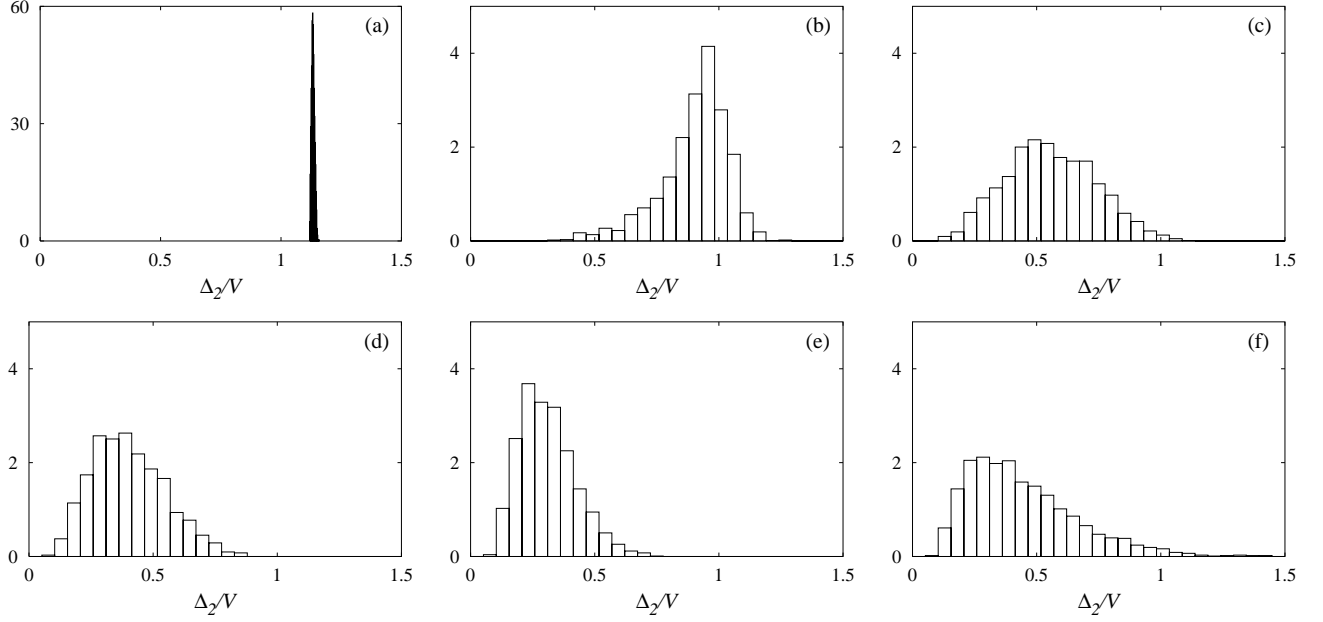


FIG. 3: Distribution of  $\Delta_2/V$  in the classical system of size  $L = 8$  for disorder strength  $W = V =$  (a) 0.01, (b) 0.1, (c) 0.2, (d) 0.3, (e) 1, (f) 5.

at  $W = V = 0.2$ . In addition, as  $W = V$  is raised, the emergence of rather disordered states in turn leads to the increase of the fluctuations of  $\Delta_2/V$ , which is reflected as well in the correlations between  $E_{M+1}$  and  $E_M$  and  $E_{M-1}$  and  $E_M$  shown in Fig. 4. In this regime the correlations are positive and increase with  $W = V$  until  $W = V = 0.2$ , keeping parallel with the broader distribution of  $\Delta_2/V$ . [Recall that  $\Delta_2 = (E_{M+1} - E_M) + (E_{M-1} - E_M)$ .] Such positive correlations may be understood via the argument that the presence of a dilute region in state  $M$ , which lowers  $E_{M+1} - E_M$ , accompanies a dense region, allowing a low cost of the electron extraction. It should be noted that large fluctuations in this regime arise from the interplay between the Coulomb interaction and the random potential.

The main feature of Region II is that essentially all the states are disordered. In this regime the disorder contributions become important in determining the electron configuration of  $M$ , alleviating the need for rearrangement due to the insertion or extraction of an electron. The fluctuations  $[E_{M-1} - E_M]$ , which increase or decrease very slightly depending on the system size, are not enough to explain the noticeable decrease of  $\Delta_2/V$  shown in Fig. 1 (b), suggesting that the correlations between them play a crucial role. Figure 4 shows that the correlations decrease to negative values. This behavior, providing an evidence for the mounting role of the random potential, can be understood as follows: In the non-interacting case  $E_{M+1} - E_M$  and  $E_{M-1} - E_M$  are simply given by  $w_{M+1}$  and  $w_M$ , respectively, where  $w_n$  is the  $n$ th smallest strength of the on-site potential in a disordered sample. The closeness of  $w_{M+1}$  and  $w_M$  gives positive correlations between them, thus leading to neg-

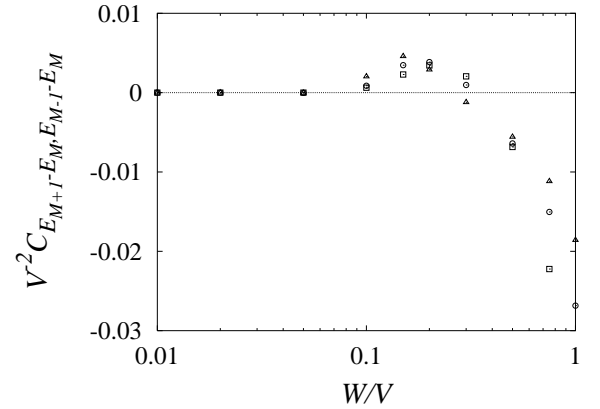


FIG. 4: Correlations between  $E_{M+1} - E_M$  and  $E_{M-1} - E_M$  in units of  $V^2$  in the classical system of size  $L = 4$  ( ),  $6$  ( ), and  $8$  ( ).

ative correlations between  $E_{M-1} - E_M$ . This argument is expected to remain valid in the presence of sufficiently weak interactions. It is remarkable that such correlations indeed begin to show up in the regime of rather strong interactions. Furthermore, as can be seen from Fig. 3 (c) and (d), the distribution of  $\Delta_2/V$  is bounded below by the minimum of  $\Delta_2/V$  given by Eq. (5), while the maximum of  $\Delta_2/V$  decreases with  $W = V$ , accounting for the corresponding decrease of the fluctuations  $\Delta_2/V$ .

Finally, one can observe that Region III is characterized by weak dependence of  $\langle \Delta_2 \rangle = V$ ,  $\Delta_2/V$ , and  $\Delta_2 = \langle \Delta_2 \rangle$  upon the disorder strength. Although fluctuations of  $E_{M+1} - E_M$  and of  $E_{M-1} - E_M$  increase with

$W=V$ , they are canceled out due to their negative correlations as disclosed in Fig. 4. It should also be noted that the inverse-compressibility distribution follows the WD form throughout this regime [see Fig. 3 (e)] while the universal relative fluctuations reported in Refs. 6 and 7 emerge only for  $W=V=1$ .

Before closing this section, we add a remark on the shape of the distribution of the inverse compressibility, which is displayed in Fig. 3 for several values of  $W=V$ . The noninteracting system follows the Pauli distribution, which changes to the WD distribution for  $0.5 < W=V < 0(1)$  as pointed out above. Further decrease to  $0.05 \leq W=V \leq 0.2$  generates quite a peculiar distribution: the asymmetric one with a peak biased to the right and a long tail in the left, which resembles neither the WD nor the Gaussian distribution. As  $W=V$  becomes even smaller, this distribution eventually reduces to the  $\delta$ -function distribution, manifesting the WC state.

### III. QUANTUM COULOMB GLASS

In this section we allow hopping of electrons between sites and investigate the corresponding quantum effects. The Hamiltonian for such a quantum Coulomb glass reads<sup>16,17</sup>

$$H = t \sum_{\langle i,j \rangle} (\hat{c}_i^\dagger \hat{c}_j + \hat{c}_j^\dagger \hat{c}_i) + \sum_i w_i \hat{n}_i + \frac{1}{2} \sum_{i \neq j} (\hat{n}_i - K) U_{ij} (\hat{n}_j - K); \quad (6)$$

where  $\hat{c}_i^\dagger/\hat{c}_i$  is the creation/annihilation operator at site  $i$  and the number operator is given by  $\hat{n}_i = \hat{c}_i^\dagger \hat{c}_i$ . The hopping of an electron is allowed only between nearest neighboring sites as indicated by the first term. We employ the HF approximation to treat the Coulomb interaction in Eq. (6), and obtain

$$H_{\text{HF}} = t \sum_{\langle i,j \rangle} (\hat{c}_i^\dagger \hat{c}_j + \hat{c}_j^\dagger \hat{c}_i) + \sum_i w_i \hat{n}_i + \sum_{i \neq j} (\hat{n}_j - K) U_{ij} \hat{n}_i + \sum_{i \neq j} \langle \hat{n}_j \rangle U_{ij} \hat{c}_i^\dagger \hat{c}_j;$$

apart from constant terms. The third and the fourth terms represent the direct and the exchange energies of the electron-electron interactions, respectively, and the angular brackets denote the expectation values with respect to the HF ground state, which should be determined in a self-consistent manner. During the iteration we use the method of potential mixing, where the averages over a few previous iterating steps are inserted into the expectation values in the Hamiltonian; this not only ensures convergence of the iteration but also helps to reduce iteration steps necessary for convergence.

We have computed the inverse compressibility up to 2000 disorder configurations for several values of the hop-

ping strength  $t=V$  and the disorder strength  $W=V$ . Figure 5 displays the distribution of the inverse compressibility for various values of  $t=V$  and  $W=V$ , together with the distribution in the corresponding classical system. For small  $W=V$  shown in Figs. 5 (a), (b), and (c), as electron hopping comes into play, the peak position of the distribution moves toward smaller values of  $\chi_2$ , with the probability for large  $\chi_2$  reduced. One can see that for  $W=V=0.1$  the presence of even very weak hopping produces a noticeable change in the distribution. Indeed the clean system ( $W=0$ ) is observed to show rapid decrease of the inverse compressibility with the increase of the hopping strength, suggesting that the decrease of the probability for large  $\chi_2$  originates from the interplay between the Coulomb interaction and hopping. Figure 5 (d), (e), and (f) corresponding to  $W=V=0.5$ , in contrast, demonstrates that the peak shifts slightly to the right and appears to saturate eventually as the hopping strength is increased. In addition, the probability for small  $\chi_2$  is suppressed and the minimum of  $\chi_2$  rises, which appears to begin at somewhat weaker disorder  $W=V=0.2$ . Recalling that such suppression in the probability for small  $\chi_2$  is also observed in the noninteracting system, we can infer that random disorder plays a crucial role here. The effects of electron hopping are also manifested by the statistics of the inverse compressibility, which is presented in Fig. 6. For  $W=V < 0.5$ , both  $\langle \chi_2 \rangle$  and  $\chi_2$  decrease with  $t=V$  due to the reduction of the probability for large  $\chi_2$ ; for  $W=V > 0.5$ , on the other hand, the suppression of small  $\chi_2$  induces slight increase of  $\langle \chi_2 \rangle$  and decrease of  $\chi_2$ , which results in overall suppression of  $\chi_2 = \langle \chi_2 \rangle$  in the whole region.

Figure 7 illustrates the interaction effects on the inverse-compressibility distribution for given hopping and disorder strength. As the interaction strength is increased, the peak in the distribution of the normalized inverse compressibility ( $\chi_2 - \langle \chi_2 \rangle = \chi_2$ ) moves to the right both in the clean case ( $W=t=1$ ) and in the dirty case ( $W=t=5$ ). Here it is of interest to notice the growth of a tail in the left side. The increase of the interaction modifies the WD-like distribution to a symmetric one and even drives the distribution into a right-biased shape at sufficiently strong interactions [see Fig. 7 (c)]. The distribution returns to a symmetric narrow one upon further increase of the interaction. Strong disorder in dirty samples, on the other hand, tends to suppress such influence of the interaction: Growth of the left tail is retarded and the distribution remains in the left-biased shape even at strong interactions.

Several experiments<sup>1,2,3</sup> reported that the distribution of the normalized inverse compressibility follows a roughly symmetric Gaussian form with non-Gaussian tails, which is very different from the WD distribution predicted by the random matrix theory. The interaction strength in those experiments is characterized by the dimensionless parameter  $r_s \sim 1$  to 2, which, via the relation  $r_s = V/(2t)$  with the filling factor  $\nu = 1/2$ , corresponds to  $V=t \sim 2$  to 5 in our model. In this interaction

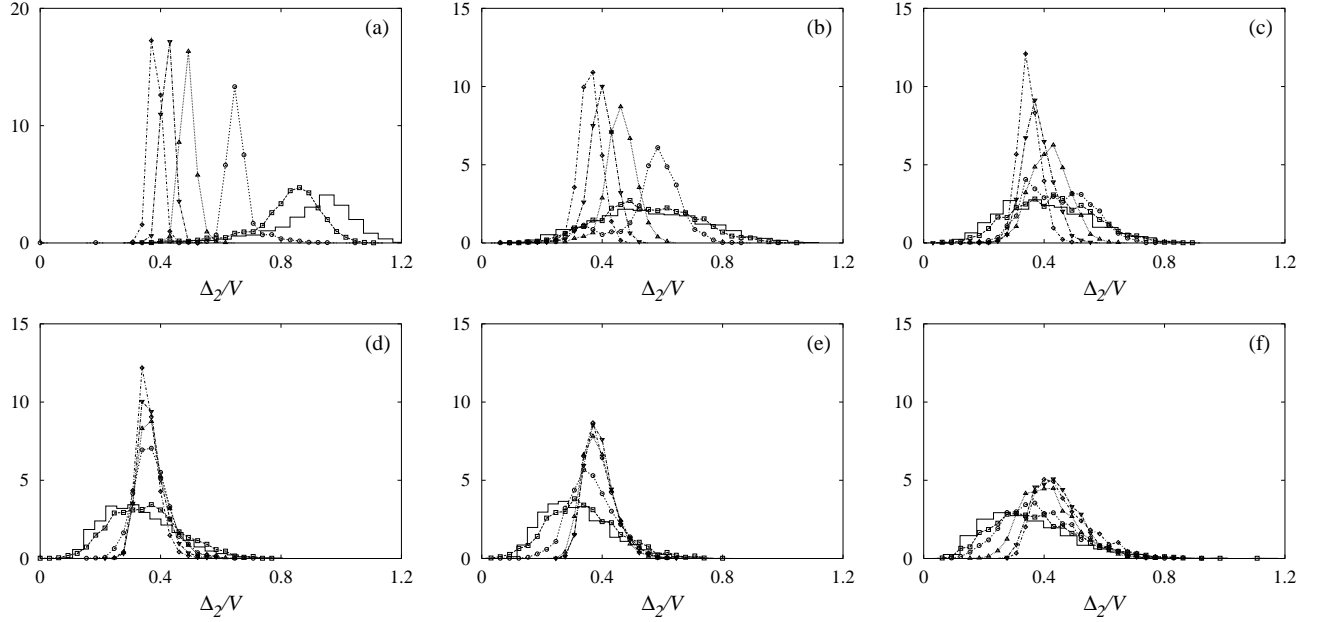


FIG. 5: Distributions of  $\Delta_2/V$  in the quantum system of  $L = 8$  for  $W=V =$  (a) 0.1, (b) 0.2, (c) 0.3, (d) 0.5, (e) 1, and (f) 2. For comparison, the distribution in the classical system ( $t=V = 0$ ) is plotted by a thick solid line in each figure. The data marked by squares, circles, triangles, inverted triangles, and diamonds correspond to the hopping strength  $t=V = 0.1; 0.5; 1; 2$ , and 10, respectively.

range and also at weaker interactions we have identified such a Gaussian-like symmetric distribution as long as disorder is sufficiently weak ( $W=V \lesssim 0.3$ ). In addition to this symmetric distribution, we have also observed an interesting asymmetric right-biased distribution with long left tails for  $0.05 < W=V < 0.2$  and  $t=V \lesssim 0.2$  [see Fig. 7 (c)]. Indeed, such an asymmetric distribution, which also appears in Fig. 3 (b) for the classical system, has been observed experimentally<sup>2</sup> in the samples with strong interactions  $r_s \gtrsim 2.1$  and rather weak disorder. [See Fig. 3 in Ref. 2.] Furthermore, we have obtained in this regime relative fluctuations smaller than the values 0.1–0.2 obtained in previous numerical calculations;<sup>1,6,7</sup> this allows one to explain the weak relative fluctuation  $\Delta_2 = \langle h_2 \rangle \approx 0.06$  observed in experiment without considering thermal broadening. All these observations thus support the conclusion that the peak spacing fluctuations in the Coulomb blockade conductance originate mainly from charging energy fluctuations.

We also investigate the effects of the interaction on the statistics of the inverse compressibility by computing the relative fluctuations, which are shown as a function of  $V=t$  for several values of  $W=t$  in Fig. 8. It is observed that particularly for intermediate disorder strengths a broad peak develops at a certain value of  $V=t$ , which turns out to increase with  $W=t$ . The decrease of  $\Delta_2 = \langle h_2 \rangle$  at sufficiently strong interactions has its origin in the fast increase of  $\langle h_2 \rangle$  as well as the decrease of  $\Delta_2$  with  $V=t$  in this regime, where the half-filling state is close to the WC state. Note here that such decrease was not observed in Ref. 8, which investigated the quarter-filled system and

reported quadratic increase of the relative fluctuations with  $V=t$  at strong interactions. In general stronger interactions are required for systems with smaller filling factors to form WC states, and accordingly it is expected that relative fluctuations begin to decrease at larger values of  $V=t$ . We thus believe that further increase of the interaction strength should yield reduction of the relative fluctuations even in the quarter-filled case.

Finally, we check the validity of the HF approximation by comparing the HF results with those obtained via exact diagonalization of the Hamiltonian in Eq. (6) for small systems. In Fig. 9 (a) and (b), which displays the statistics of  $\Delta_2$  obtained via the two methods in the system of  $L = 4$ , one can see that the HF results are in good agreement with the exact ones except for some parameter regions: For  $V=t > 1$ , observed in Fig. 9 (a) is that the HF approximation overestimates  $\langle h_2 \rangle$  for small  $W=V (\lesssim 0.3)$ . Figure 9 (b) also shows such overestimation of the fluctuations in the HF approximation for the intermediate disorder strength  $0.1 \lesssim W=V \lesssim 1$  and  $V=t > 1$ . The distribution function plotted in Fig. 9 (c) and (d) provides a clue to the overestimation: For  $W=V = 0.2$  corresponding to moderate disorder, the HF approximation generates more frequently large values of  $\Delta_2$  and hardly changes the minimum of  $\Delta_2$ , resulting in the overestimation of both  $\langle h_2 \rangle$  and  $\Delta_2$ . On the other hand, for smaller  $W=V = 0.1$  the overall distribution merely shifts to the right with the shape almost unchanged. Accordingly, whereas the HF approximation tends to give larger values of  $\langle h_2 \rangle$ , rather accurate values are obtained for  $\Delta_2$  in the case of small  $W=V$ , as shown in Fig. 6.

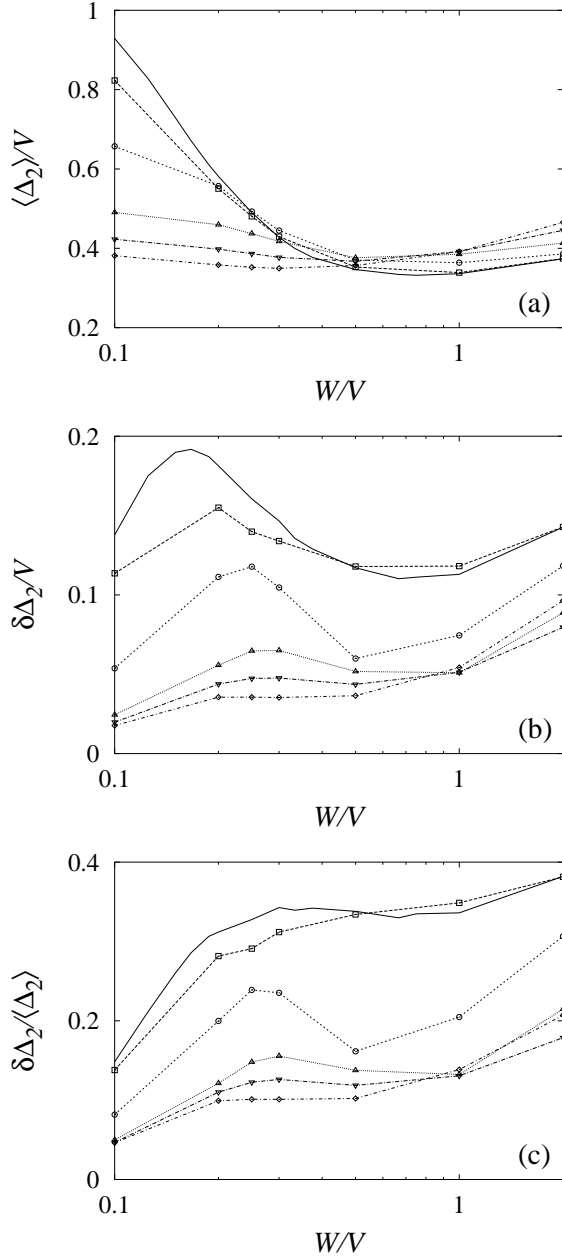


FIG. 6: (a) Average, (b) fluctuations, and (c) relative fluctuations of the inverse compressibility as functions of  $W/V$  in the quantum system of size  $L = 8$ . The data marked by squares, circles, triangles, inverted triangles, and diamonds correspond to the hopping strength  $t=V = 0.1; 0.5; 1; 2$ , and  $10$ , respectively, while the thick lines represent the data in the classical limit ( $t=V = 0$ ).

#### IV. EFFECTS OF MAGNETIC FIELDS

In this section we examine the effects of magnetic fields on the distribution and fluctuations of the inverse compressibility. Electrons hopping in applied magnetic fields acquire additional phases, leading to the kinetic term in

the Hamiltonian

$$H_K = t \sum_{\langle i,j \rangle} (e^{iA_{ij}} c_i^\dagger c_j + e^{-iA_{ji}} c_j^\dagger c_i) \quad (7)$$

The phase  $A_{ij}$  associated with the hopping between sites  $i$  and  $j$  is given by

$$A_{ij} = \begin{cases} 2\pi f_{\hat{y}} & \text{for } j = i + \hat{x} \\ 0 & \text{for } j = i + \hat{y} \end{cases}$$

in the Landau gauge, where  $f = B \phi_0 / 2\pi$  is the frustration parameter in the presence of a uniform transverse magnetic field  $B = B\hat{z}$ . We also adopt the free boundary conditions, which are convenient for describing the system with arbitrary values of the frustration parameter (i.e., under arbitrary magnetic fields) without any mismatch on the boundaries. Periodic boundary conditions in general cannot avoid such mismatch except for rather low-lying rational values of the frustration restricted by the system size.

Some experimental groups<sup>1,3</sup> have measured the conductance peak spacing in the presence of finite magnetic fields, reporting that the distribution of  $\nu_2$  remains symmetric and Gaussian-like, as in the case of zero magnetic field, with slightly smaller width:  $(\nu_2 = h \nu_2 / e)_{B=0} (\nu_2 = h \nu_2 / e)_{B \neq 0}^{-1} = 1.2 \pm 0.1$ .<sup>3</sup> Note that those experiments probed the weak-field regime: The magnetic flux per electron in units of the flux quantum roughly amounts to  $0.08$ ,<sup>1</sup> or  $0.002$  to  $0.04$ .<sup>3</sup>

Motivated by this, we first concentrate on the weakly frustrated systems, where magnetic fields are weak enough not to change significantly the characteristics around the Fermi levels of corresponding noninteracting clean systems. Such a case is given by the frustration range  $0 < f < f_{d1}$ , where  $f_{d1}$  is the smallest nonzero value of the degenerate frustration defined below. We then consider the system with large values of the frustration, especially the fully frustrated system with  $f = 1/2$ .

For clear identification of the magnetic-field effects, we first investigate the system of free electrons on a lattice, in the presence of a magnetic field. It is well known that in two dimensions the system is described by Harper's equation, displaying the characteristic spectrum of a very complex pattern.<sup>18</sup> In Fig. 10 we show the single-particle energy spectrum and the corresponding inverse compressibility in the half-filling case. It is observed that the Fermi level becomes degenerate at some values of the frustration, leading the inverse compressibility to vanish. As the system size grows, the number of such degenerate frustrations, denoted by  $f_d$ , increases rapidly and they spread out over the whole interval  $[0; 1/2)$  except near the full frustration ( $f = 1/2$ ).

A recent study<sup>7</sup> has revealed that in the absence of the magnetic field the degeneracy at the Fermi level in a free-electron system affects the inverse compressibility and its fluctuations. The single-particle energies in the

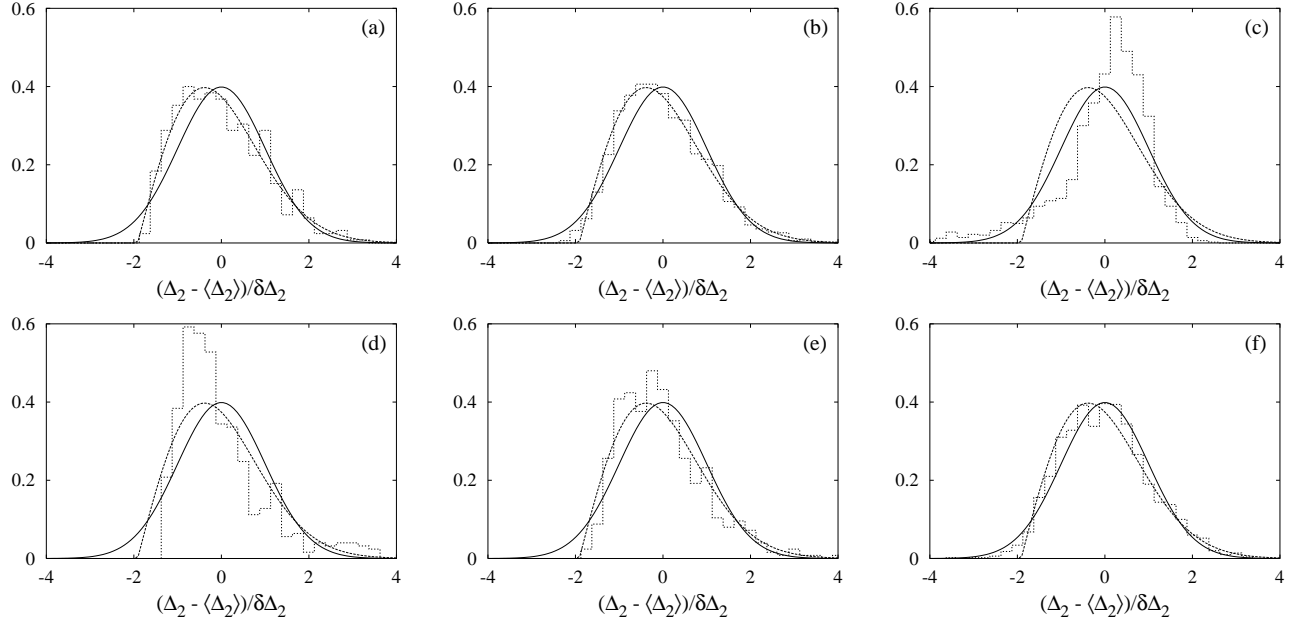


FIG. 7: Distributions of the normalized inverse compressibility in the quantum system of  $L = 8$  for  $W/t = 1$  and  $V/t =$  (a) 0.1, (b) 1, (c) 10; for  $W/t = 5$  and  $V/t =$  (d) 0.1, (e) 1, (f) 10. The solid and the dashed curves represent the best fit to the normalized Gaussian and to the WD distributions, respectively.

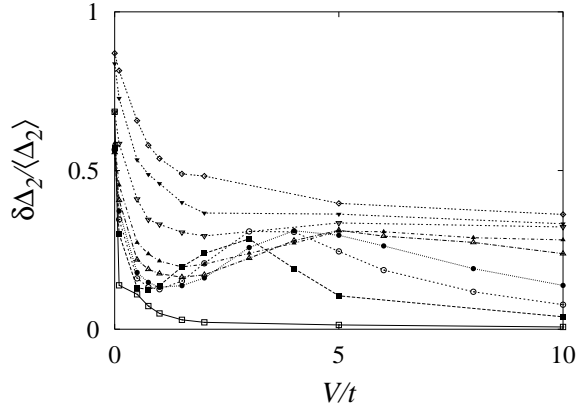


FIG. 8: Relative fluctuations of the inverse compressibility versus  $V/t$  in the quantum system of  $L = 8$  for various values of  $W/t = 0.1$  ( ),  $0.5$  ( ),  $0.75$  ( ),  $1$  ( ),  $1.5$  ( ),  $2$  ( ),  $4$  ( ),  $6$  ( ), and  $10$  ( ).

system are given by

$$\epsilon_{nm} = -2t \cos \frac{n\pi}{L+1} + \cos \frac{m\pi}{L+1} \quad (8)$$

with  $n$  and  $m$  being integers from 1 to  $L$ . Accordingly, there are  $L$  degenerate states with  $(n; m) = (1; L); (2; L-1); \dots; (L; 1)$  at the Fermi level. This degeneracy yields finite average inverse compressibility together with non-vanishing relative fluctuations in the free-electron limit of the interacting disordered system.<sup>7</sup> Such observation leads to a natural question whether the same phenomena { relatively small inverse compressibility and non-

vanishing relative fluctuations } remain at nonzero degenerate values of the frustration and how the distribution of the inverse compressibility changes with them magnetic field. An answer to such questions are given below. In general, for large systems where the set of the degenerate frustration becomes very dense, the statistics of the inverse compressibility is expected to remain qualitatively unchanged irrespective of the frustration, except around  $f = 1/2$ .

#### A. Weakly Frustrated System

We now examine the effects of weak magnetic fields on the statistics of the inverse compressibility. Recalling that the influence of the magnetic field enters only in the hopping term as an additional phase, we can infer that the magnetic-field effects are not prominent in the system with small hopping strength. Indeed, for  $W/t > 2$  or  $V/t > 2$ , no distinctive change has been found numerically, at least in the presence of weak magnetic fields.

Figure 11 shows the dependence of  $\chi_{2i=t}$  on the frustration: The magnetic field initially enhances  $\chi_{2i=t}$ , which is expected from the increase of  $\chi_2$  with  $f$  in the free-electron system. As  $f$  approaches  $f_{d1}$ , the first nonzero degenerate frustration in the corresponding non-interacting clean system, however,  $\chi_{2i=t}$  decreases to a value which is close to the zero-frustration value. Level repulsion due to random disorder smoothes out the dependence on  $f$ , especially at the degenerate frustration.

On the other hand, fluctuations of the inverse compressibility show different behaviors with the frustration,



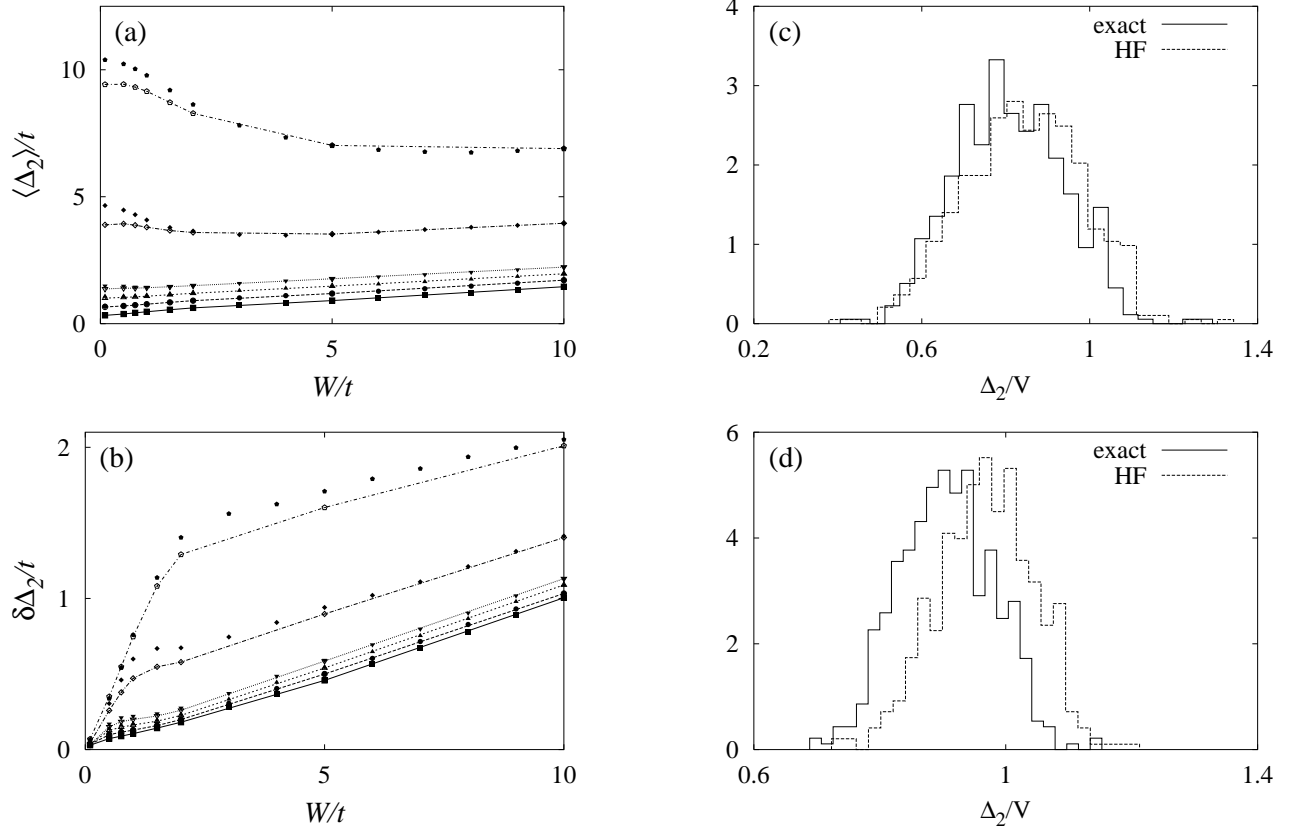


FIG. 9: Comparison of the HF results (filled symbols) and the exact ones (empty symbols with lines) for (a) the average and (b) fluctuations of the inverse compressibility in the quantum system of  $L = 4$  for various values of  $V/t = 0.5; 1; 1.5; 2; 5$ , and 10 from below; comparison of the inverse-compressibility distribution for  $V/t = 10$  and  $W/V =$  (c) 0.2 and (d) 0.1. The discrepancy between the two results is considerable in (d).

depending on the strength of the interaction and disorder. In the system with weak disorder [see Fig. 12 (a) (c) for  $W/t = 0.5$ ],  $\Delta_2/t$  versus  $f$  exhibits two minima for weak interactions  $V/t < 2$ , which turn into a single minimum as the interaction is increased; these features, however, become less pronounced with the increase of the system size. For strong disorder ( $W/t = 2$ ) shown in Fig. 12 (d), (e), and (f), the peculiar structure observed in the weak-disorder regime fades away and  $\Delta_2/t$  tends to decrease with the frustration, particularly in large systems.

From the distribution of  $\Delta_2$  presented in Fig. 13, one can get a hint as to the origin of the behavior of fluctuations in the weakly disordered system. Turning on the magnetic field initially suppresses the appearance of small  $\Delta_2$  and thus reduces fluctuations regardless of the interaction strength, as can be observed in Fig. 13 (a) and (c). Further increase of  $f$ , however, raises significantly the portion of large  $\Delta_2$  in the presence of weak interactions, inducing large fluctuations [see Fig. 13 (b)]. When  $f$  exceeds the value at which  $\Delta_2/t$  reaches its maximum, the reverse process takes place, producing another minimum of  $\Delta_2/t$ . In contrast, strong interactions seem to suppress such extension of the distribution to the

large- $\Delta_2$  region, leading to a curve with one minimum for  $\Delta_2/t$ .

To examine the relation between different responses to the magnetic field and localization properties, we introduce the participation ratio and the inverse participation number (IPN)  $P^{-1}(\cdot)$ :

$$P^{-1}(\cdot) = \frac{N_e^2}{\sum_i \langle \rho_i \rangle^2} \quad (9)$$

$$P^{-1}(\cdot) = \frac{L^2}{X} \sum_i |j_i(\cdot)|^4; \quad (10)$$

where  $N_e$  is the total number of electrons,  $\langle \rho_i \rangle$  is the expectation value of the electron density at site  $i$ , and  $j_i(\cdot)$  is the probability amplitude for the single-particle state  $j$  at site  $i$ . The participation ratio is equal to unity in the state with a uniform density profile and decreases as the electron configuration becomes modulated or localized, eventually reaching the minimal value of the filling factor  $N_e/L^2$  in the limit that all the electrons are located at the  $N_e$  sites.<sup>19</sup> The IPN, on the other hand, assumes unity for the level localized at one site and decreases as the state becomes delocalized, approaching its minimal value  $L^{-2}$  in the opposite limit of the uniformly extended

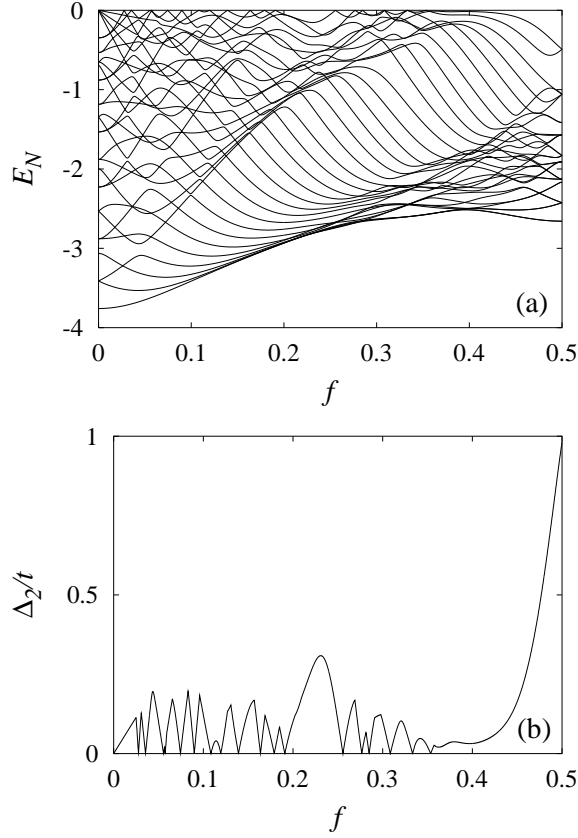


FIG. 10: (a) Single-particle energy spectrum and (b) the inverse compressibility versus frustration in the half-filled non-interacting clean system of size  $L = 8$ . Since the spectrum possesses reflection symmetry with respect to the  $E = 0$  line, only lower half of the spectrum is shown here.

state.<sup>20</sup>

We use these measures to characterize localization or modulation of the half-filled state  $M_i$  and search for the possible relation with the inverse compressibility, which reveals that for given frustration the participation ratio in general has negative correlations with the inverse compressibility: The smaller the inverse compressibility, the larger the participation ratio and vice versa. This observation indicates that the electron profiles in the samples with smaller values of  $\Delta_2$  tend to be uniform and thus explains the increase of  $\Delta_2$  in the samples displaying relatively small  $\Delta_2$  since such uniform profiles should be sensitive to the change in frustration. Localized states, on the other hand, are rather insensitive to frustration, and accordingly, the inverse compressibility in a sample with large  $\Delta_2$  remains unchanged. To be more definite in the electron state, we have also calculated the IPN at the Fermi level and observed positive correlations between the IPN and the inverse compressibility, thus confirming the above argument. In the case that hopping is dominant over the interaction and disorder, the samples mostly have large values of the participation ratio and low values of the IPN at the Fermi level, implying sensi-

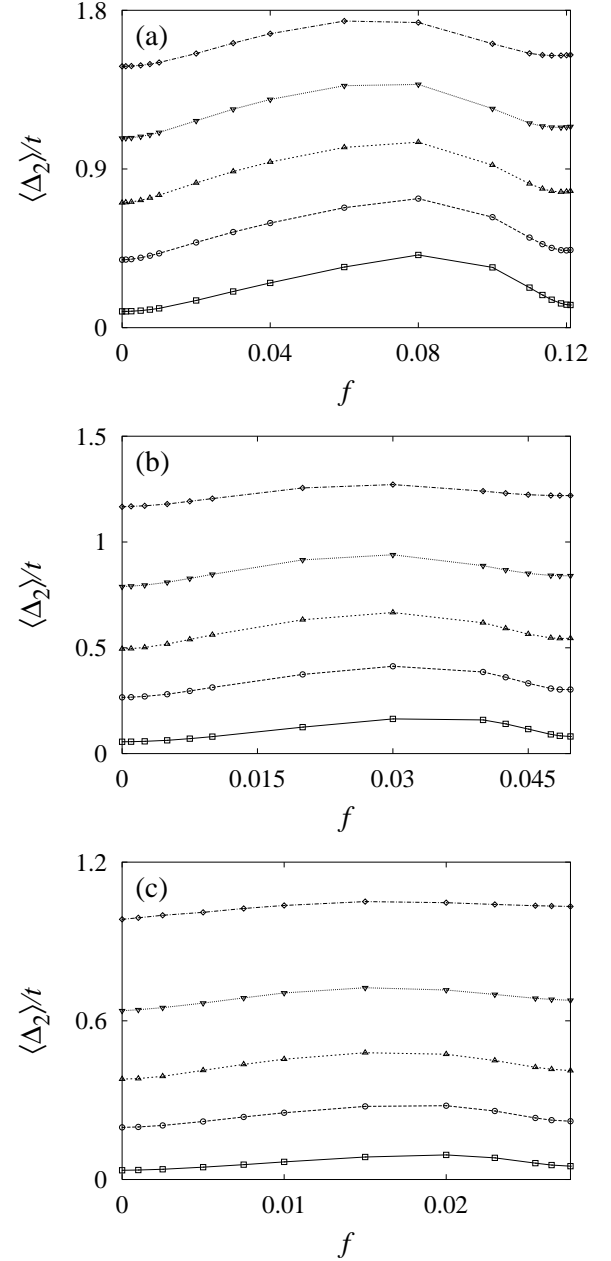


FIG. 11: Average inverse compressibility versus frustration  $f$  in the range  $[0; f_{d1}]$  for various values of  $V/t = 0$  ( $\diamond$ ),  $0.5$  ( $\nabla$ ),  $1$  ( $\triangle$ ),  $1.5$  ( $\circ$ ), and  $2$  ( $\square$ ) in the system of size  $L =$  (a) 4, (b) 6, and (c) 8. The disorder strength  $W/t$  is set to be 0.5.

tivity to frustration. Variations of the sensitivity over the samples lead to the increase of width of the distribution.

As  $f$  approaches  $f_{d1}$ , the distribution reverses its behavior, restoring that at  $f = 0$ . However, it should be noted that the distributions at  $f = 0$  and at  $f = f_{d1}$  are not exactly the same. Rather, the distribution at  $f = f_{d1}$  is similar to the one at  $f = 0.005$ . Such difference between the distributions at different degenerate frustrations may be attributed to the difference of the degree of degeneracy: At  $f = 0$  the system has the  $L$ -

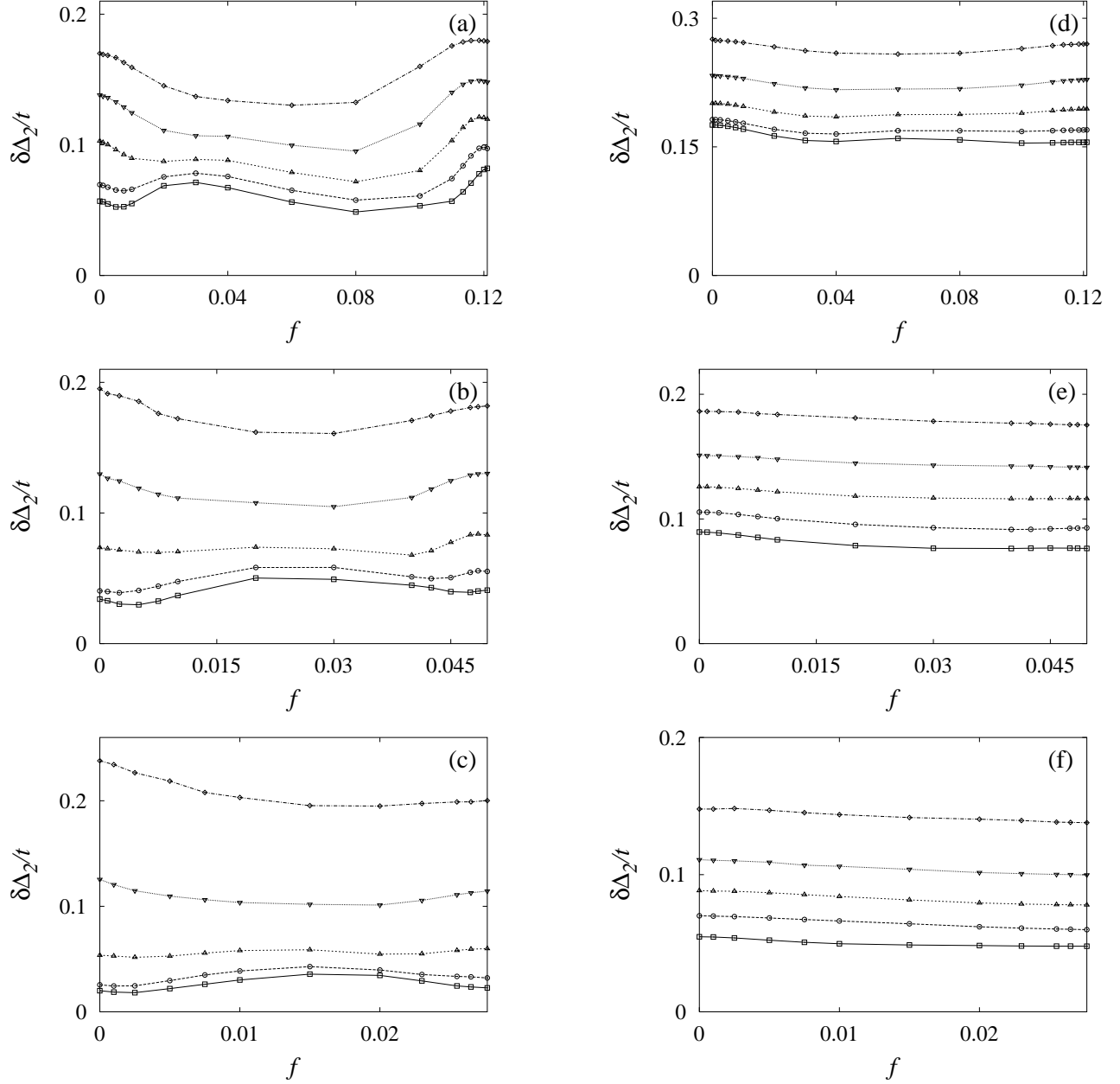


FIG. 12: Fluctuations of the inverse compressibility versus frustration for various values of  $V/t = 0$  ( $\square$ ),  $0.5$  ( $\circ$ ),  $1$  ( $\triangle$ ),  $1.5$  ( $\diamond$ ), and  $2$  ( $\nabla$ ) in the weakly disordered system ( $W/t = 0.5$ ) of size  $L =$  (a) 4, (b) 6, (c) 8 and in the strongly disordered system ( $W/t = 2$ ) of size  $L =$  (d) 4, (e) 6, (f) 8.

fold degeneracy at half-filling but at  $f = f_{d1}$  two-fold degeneracy is present, as can be seen in Fig. 10 (a). Since large degeneracy favors a smaller value of  $\chi_2$  even in the presence of the interaction and disorder, the probability for small  $\chi_2$  at  $f = 0$  is higher than that at  $f = f_{d1}$ , which is verified in numerical calculations.

To get more insight for large fluctuations at the degenerate frustration in relation to the localization property, we have computed the average participation ratio  $\langle h_i \rangle$ , which is plotted as a function of  $f$  for various interaction strengths in Fig. 14. The conspicuous decrease in

$\langle h_i \rangle$  near the degenerate frustration signals an increase in spatial modulation or localization of the total electron density. Indeed in a perfectly clean system the participation ratio is exactly equal to unity, irrespective of the frustration. As disorder is introduced,  $\langle h_i \rangle$  diminishes faster at the degenerate frustration. Such spatial localization at the degenerate frustration or delocalization at non-degenerate frustration are believed to be related with the pattern of interference of electrons scattered at impurities: Moving around the lattice under the magnetic field, the electrons acquire additional phases. At the de-

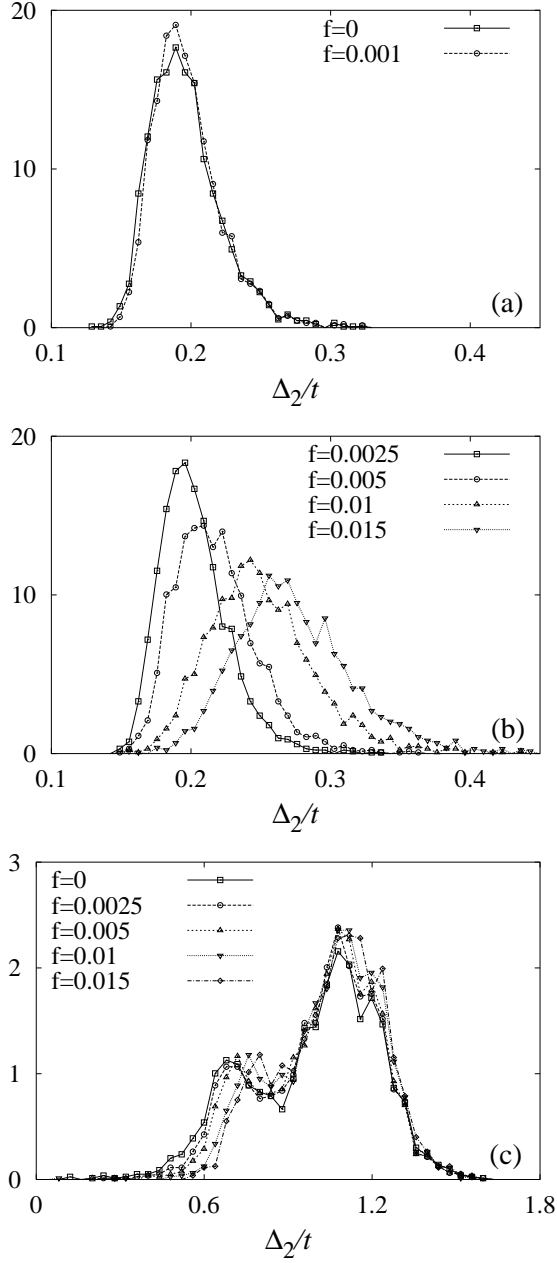


FIG. 13: Distribution of the inverse compressibility in the system of size  $L = 8$  for  $W = t = 0.5$ . The interaction strength is given by  $V = t = 0.5$  in (a) and (b) and  $V = t = 2$  in (c); the frustration  $f$  is varied from 0 to  $f_{d1}$ .

generate frustration such phases are expected to enhance the constructive interference. In connection with the degeneracy we can imagine linear combinations of degenerate states at the Fermi level; any combination will be an eigenstate of the clean system, and among them we can choose more modulated or localized one which leads to less energy in the presence of disorder. At the non-degenerate frustration such choice is not possible, yielding rather extended states.

The sensitivity of electron states to disorder at the de-

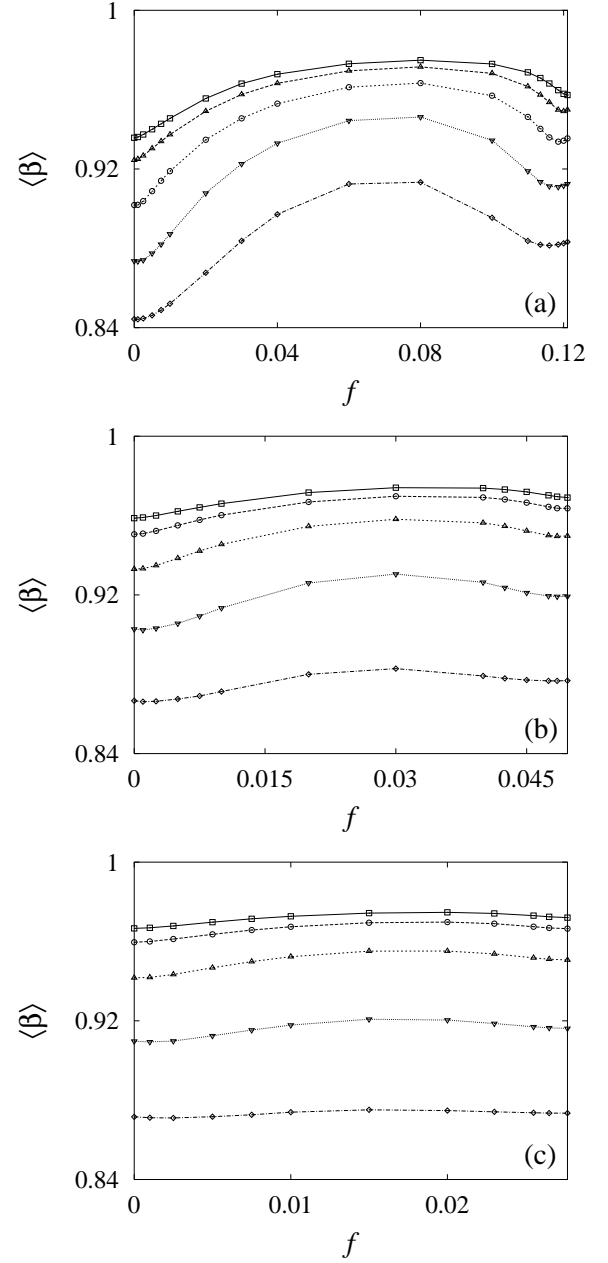


FIG. 14: Average participation ratio versus frustration in the range  $[0; f_{d1}]$ . The system has the size  $L =$  (a) 4, (b) 6, (c) 8 together with the interaction  $V = t = 0$  ( ), 0.5 ( ), 1 ( ), 1.5 ( ), and 2 ( ). The disorder strength is given by  $W = t = 0.5$ .

generate frustration in turn generates larger fluctuations of the inverse compressibility over the samples. In Ref. 5 the enhanced fluctuations of the inverse compressibility were also attributed to localization of the wavefunctions around the edge of the dot. Here we stress that our argument is not restricted merely to the half-filling case which gives fairly high degeneracy at  $f = 0$ . Figure 10 (a) shows that there also exist many degenerate states at  $f = 0$  at other fillings.

We conclude this section with some remarks on the

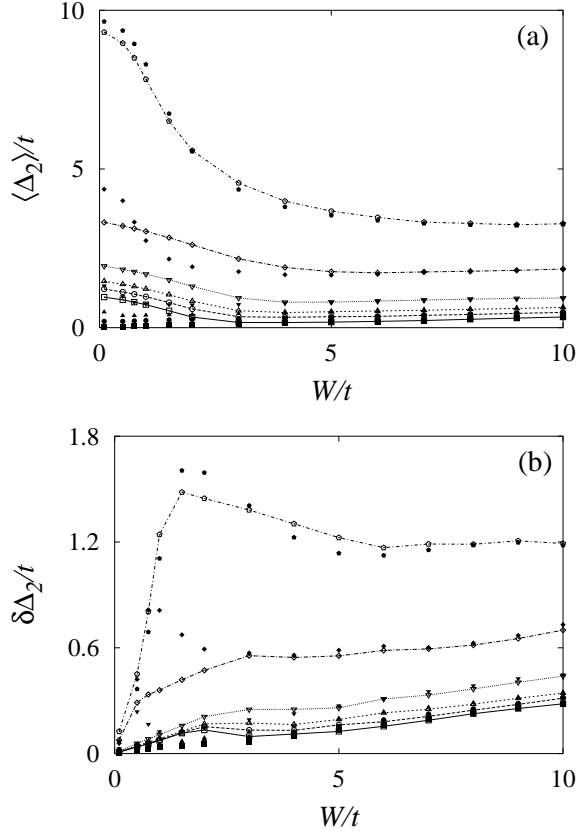


FIG. 15: (a) Average and (b) fluctuations of the inverse compressibility versus  $W/t$  at  $f = 1/2$  (empty symbols with lines) and at  $f = 0$  (filled symbols) in the system of size  $L = 8$  for various values of  $V/t$ . The data marked by squares, circles, triangles, inverted triangles, diamonds, and pentagons correspond to  $V/t = 0, 0.5, 1, 2, 5, 10$ , respectively.

comparison with the existing experiment. For the interaction and disorder which are sufficiently strong but not so strong to overwhelm quantum effects, the fluctuations are observed to diminish with the frustration  $f$ , provided that  $f > f_{d1}$ . This leads to similar decrease in relative fluctuations, even for weak disorder and interaction, owing to the increase in  $h_{2i}$ . This result agrees quite well with the experimental results mentioned in the beginning of this section. Furthermore, the structure of the inverse compressibility distribution has been found not to change appreciably, which also coincides with the experimental observation.

### B. Fully Frustrated System

In the previous section, we have examined the effects of weak magnetic fields, up to the first degenerate frustration  $f_{d1}$ , on fluctuations of the inverse compressibility. The arguments in the previous section as to the fluctuations at degenerate and non-degenerate frustrations seem to be applicable beyond  $f_{d1}$  as well. However, as the sys-

tem size grows, the degenerate frustrations proliferate in number to spread over the entire region of the frustration and the energy splitting by the magnetic field at the Fermi level also shrinks. Accordingly, no distinctive difference is expected to appear in the distribution of  $\Delta_2$  at degenerate and non-degenerate frustrations. A remarkable exception happens at the full frustration ( $f = 1/2$ ), where quite large energy spacing is induced at the Fermi level in the noninteracting clean system (see Fig. 10). For even  $L$ , the energy spacing reads

$$\frac{p}{4} - \frac{L}{2(L+1)} \cos \frac{\pi}{2(L+1)}; \quad (11)$$

which decreases to zero in the thermodynamic limit ( $L \rightarrow \infty$ ). Nevertheless, for moderate  $L$  the finite spacing given by Eq. (11) discerns the full frustration from other frustration values, yielding qualitative difference in the distribution even for strong interactions.

The average inverse compressibility and its fluctuations are displayed in Fig. 15. For  $V/t = 2$  and  $5$ , one can notice the disappearance of both the lumps in  $h_{2i=t}$  and the overshoots in  $\Delta_2=t$ , which develop at weak disorder and strong interactions in the unfrustrated system ( $f = 0$ ). In Secs. II and III, both the lumps in  $h_{2i}$  and the overshoots in  $\Delta_2$  have been found to have their origin in the WC states due to the Coulomb interaction. Accordingly, the disappearance of such lumps and overshoots implies that strong magnetic fields suppress the interaction effects on the electron distribution. To look into the distribution of the electrons, we have compared the average participation ratio at  $f = 0$  and that at  $f = 1/2$  in Fig. 16. It is observed that the latter,  $h_{i_{f=1/2}}$ , is always larger than the former,  $h_{i_{f=0}}$ , with the difference significant for  $2 \leq V/t \leq 5$ . Furthermore,  $h_{i_{f=1/2}}$  does not vary much with the interaction, up to  $V/t = 2$ ; even for  $V/t = 5$ , its values are not so different from the values for  $V/t = 0$ . We thus conclude that the full frustration restrains the modulation of electrons induced by the repulsive Coulomb interaction between electrons and suppresses its influence on the fluctuations of the inverse compressibility.

To verify the suppression of the Coulomb interaction beyond the HF approximation, we compute the participation ratio as a function of the frustration parameter via the exact diagonalization method in the clean system with a single impurity of strength  $W/t = 1$ , located at a corner of the  $4 \times 4$  lattice, and plot the results for various values of  $V/t$  in Fig. 17. Note that small values of the participation ratio indicate the formation of the WC-like states due to interactions. We have intentionally inserted an impurity in the system in order to eliminate the degeneracy, which allows the two (degenerate) WC states to superpose and may keep the participation ratio still larger even when the electrons form a Wigner crystal. At  $f = 0$  and other degenerate frustration values, the average participation ratio is clearly shown to decrease with the interaction; even rather weak interactions lead

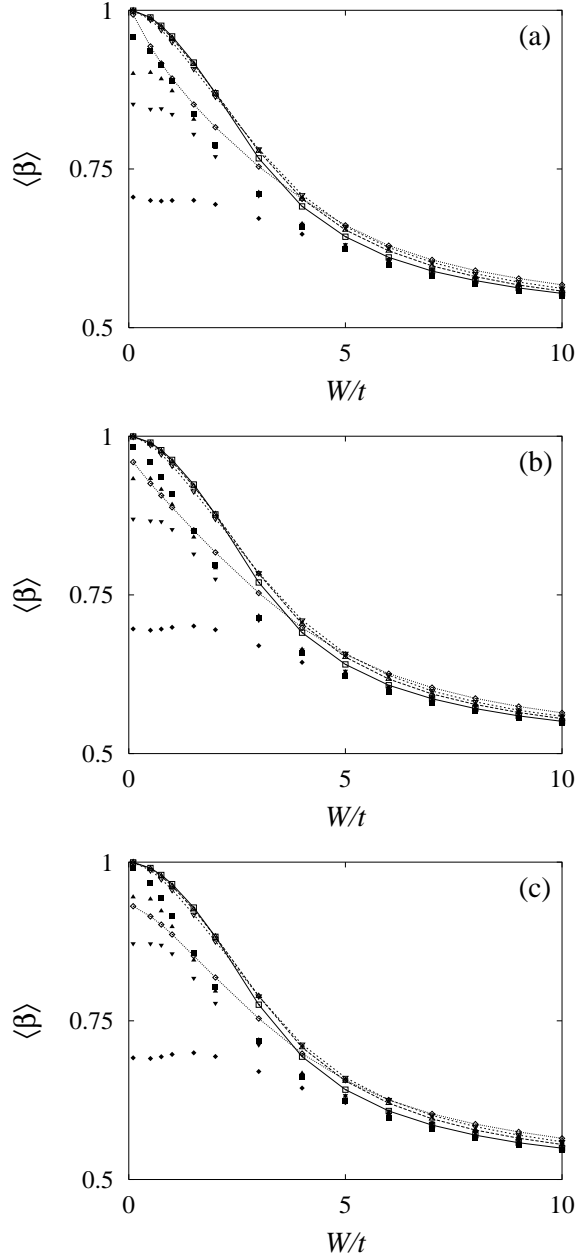


FIG. 16: Average participation ratio versus  $W/t$  at  $f = 1/2$  (empty symbols with lines) and  $f = 0$  (filled symbols) in the system of size  $L =$  (a) 4, (b) 6, (c) 8 for various values of  $V/t$ . The symbols are the same as those in Fig. 15.

to appreciable reduction in the participation ratio. At the full frustration, in contrast, the participation ratio does not reduce much even in the presence of substantial interactions, indicating that the fully frustrated system is reluctant to be in a WC state and thus confirming the above HF results.

Figure 18 compares the distribution of  $\rho_2$  at  $f = 0$  and that at  $f = 1/2$ . For  $V/t = 2$  and  $W/t = 0.5$ , shown in Fig. 18(a), the width of the distribution at  $f = 1/2$  is much reduced compared with that at  $f = 0$ . Here the

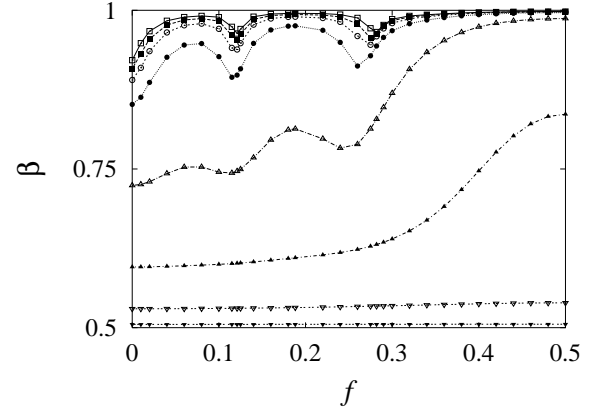


FIG. 17: Average participation ratio versus the frustration  $f$  in the system of size  $L = 4$  with a single impurity of strength  $W/t = 1$ , located at a corner of the lattice, for various values of  $V/t = 0.1$  (○),  $0.5$  (□),  $1$  (△),  $2$  (◇),  $5$  (×),  $10$  (\*),  $20$  (○), and  $50$  (□).

ubiquity of large values of  $\rho_2$  at  $f = 1/2$  comes not from the Coulomb charging energy but from the large single-particle energy splitting due to the full frustration. On the other hand, for  $V/t = 0.5$  and  $W/t = 2$ , Fig. 18(b) shows a wider distribution at  $f = 1/2$ , which may be attributed to the fluctuations of the degenerate states just above and below the Fermi level: The energies of the degenerate states fluctuate severely according to the disorder configurations, resulting in large fluctuations of the inverse compressibility.

We conclude this section with a comment on the validity of the HF approximation at  $f = 1/2$ . As observed in Fig. 17, the effects of the full frustration survive even in the presence of rather strong interactions, with the strength up to  $V/t = 10$ . Such effects are, however, not disclosed in the average and fluctuations of the inverse compressibility calculated via the HF method (see Fig. 15 for  $V/t = 10$ ). Further, the average participation ratio obtained within the HF approximation in the same system as in Fig. 17 turns out to display considerable discrepancy at  $V/t = 10$ , which strongly suggests that the HF approximation breaks down for strong interactions  $V/t \gtrsim 10$ .

## V. SUMMARY

We have studied numerically the inverse compressibility and its fluctuations in two-dimensional Coulomb glasses, with emphasis on the quantum effects associated with electron hopping as well as the frustration effects due to applied magnetic fields. For a systematic study of this problem, we have begun with the corresponding classical system, revealing the detailed dependence of the inverse compressibility fluctuations on the interaction and random disorder. Then the effects of electron hopping on the distribution of the inverse com-

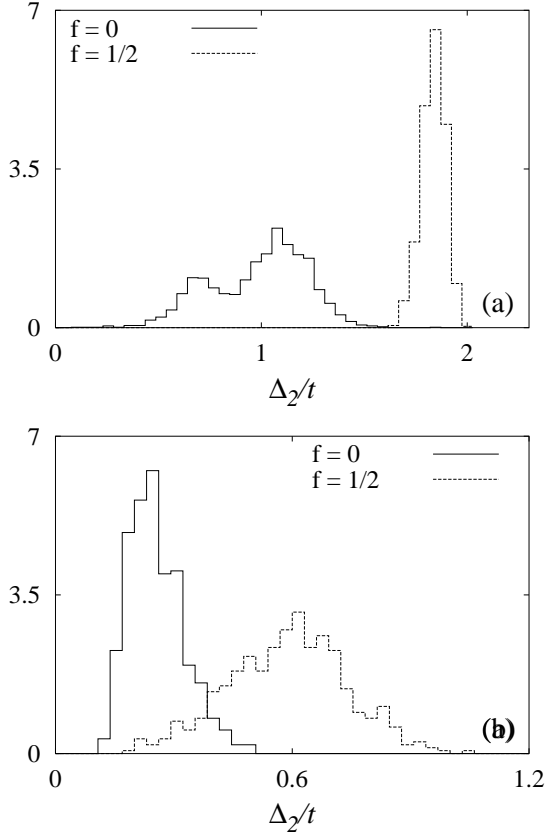


FIG. 18: Distribution of the inverse compressibility at  $f = 0$  and  $f = 1/2$  for (a)  $V/t = 2$  and  $W/t = 0.5$ ; (b)  $V/t = 0.5$  and  $W/t = 2$ .

compressibility have been examined, particularly with regard to the interplay with the interaction and disorder. The results, obtained mostly via the Hartree-Fock approxi-

mation, have been compared with those of existing experiments as well as of previous numerical studies: In addition to the symmetric Gaussian distribution with non-Gaussian tails, we have observed, in a sufficiently clean sample with strong interactions, a peculiar right-biased distribution of the inverse compressibility, which was indeed reported in experiment under similar situations. Realization of even cleaner samples, where such an unusual distribution may be attainable with rather weak interactions, is thus expected to confirm the validity of our results and to clarify the role of interactions. Remarkably, the relative fluctuations have been found to decrease eventually as the interaction strength is increased. This is contrary to the quadratic interaction dependence of the fluctuations, suggested in a previous numerical study.

We have next investigated the effects of magnetic fields on the distribution and fluctuations of the inverse compressibility. Weak frustration generally suppresses the fluctuations; in a clean sample with weak interactions, however, fluctuations are enhanced in some range of the frustration. The difference in responses to the magnetic fields has been discussed in relation to localization properties, which provides a good explanation for the effects of the magnetic fields on the distribution of the inverse compressibility. Finally, strong frustration has been observed to suppress the effects of the interaction.

#### Acknowledgments

This work was supported in part by the Ministry of Education through the BK21 Project (MLMYC) and by the Korea Science and Engineering Foundation through the Center for Strongly Correlated Materials Research (GSJ).

- <sup>1</sup> U. Sivan, R. Berkovits, Y. Aloni, O. Pius, A. Auerbach, and G. Ben-Yoseph, Phys. Rev. Lett. 77, 1123 (1996).
- <sup>2</sup> F. Simmel, T. Heinzl, and D. A. Wharam, Europhys. Lett. 38, 123 (1997); F. Simmel, D. A. Busch-Magder, D. A. Wharam, M. A. Kastner, and J. P. Kotthaus, Phys. Rev. B 59, R10441 (1999).
- <sup>3</sup> S. R. Patel, S. M. Cronenwett, D. R. Stewart, A. G. Huibers, and C. M. Marcus, Phys. Rev. Lett. 80, 4522 (1998).
- <sup>4</sup> Ya. M. Blanter, A. D. Mirlin, and B. A. Muzikantskii, Phys. Rev. Lett. 78, 2449 (1997).
- <sup>5</sup> S. Levit and D. Orgad, Phys. Rev. B 60, 5549 (1999).
- <sup>6</sup> A. A. Koulakov, F. G. Pikus, and B. I. Shklovskii, Phys. Rev. B 55, 9223 (1997).
- <sup>7</sup> G. S. Jeon, S. W. U, M. Y. Choi, and H.-W. Lee, Phys. Rev. B 59, 2841 (1999).
- <sup>8</sup> P. N. Walker, G. Montambaux, and Y. Gefen, Phys. Rev. B 60, 2541 (1999).
- <sup>9</sup> R. O. Vallejos, C. H. Lewenkopf, and E. R. Mucciolo, Phys. Rev. Lett. 81, 677 (1998).
- <sup>10</sup> Y. A. Izhassid, Ph. Jacquod, and A. Wobst, Phys. Rev. B 61, R13357 (2000).
- <sup>11</sup> S. Ilani, A. Yacoby, D. Mahalu, and H. Shtrikman, Phys. Rev. Lett. 84, 3133 (2000).
- <sup>12</sup> D. S. Duncan, D. Goldhaber-Gordon, R. M. Westervelt, K. D. Maranowski, and A. C. Gossard, Appl. Phys. Lett. 77, 2183 (2000).
- <sup>13</sup> Y. Avishai, D. Berend, and R. Berkovits, Phys. Rev. B 59, 10707 (1999).
- <sup>14</sup> N. B. Zhitenev, R. C. Ashoori, L. N. Pfeiffer, and K. W. West, Phys. Rev. Lett. 79, 2308 (1997).
- <sup>15</sup> A. L. Efros and B. I. Shklovskii, J. Phys. C 8, L49 (1975); A. L. Efros, J. Phys. C 9, 2021 (1976); M. Sarvestani, M. Schreiber, and T. Vojta, Phys. Rev. B 52, R3820 (1995).
- <sup>16</sup> Epperlein, M. Schreiber, and T. Vojta, Phys. Rev. B 56, 5890 (1997).
- <sup>17</sup> G. S. Jeon, S. W. U, H.-W. Lee, and M. Y. Choi, Phys. Rev. B 59, 3033 (1999).
- <sup>18</sup> D. R. Hofstadter, Phys. Rev. B 14, 2239 (1976); J. B. Sokoloff, Phys. Rep. 126, 189 (1985).
- <sup>19</sup> P. N. Walker, Y. Gefen, and G. Montambaux, Phys. Rev.

Lett. 82, 5329 (1999).

<sup>20</sup> For a generalization to the interacting case, see Ref. 17.